# Reactive oxygen species and antimicrobial peptides are sequentially produced in silkworm midgut in response to bacterial infection

Rui-Juan Wang[a,1], Kangkang Chen[a,1], Long-Sheng Xing[b], Zhe Lin[b], Zhen Zou[b,c,**], Zhiqiang Lu[a,d,*]

[a] Department of Entomology, College of Plant Protection, Northwest A&F University, Yangling, Shaanxi, China
[b] State Key Laboratory of Integrated Management of Pest Insects and Rodents, Institute of Zoology, Chinese Academy of Sciences, Beijing, China
[c] Key Laboratory of Vector Biology and Pathogen Control of Zhejiang Province, Huzhou University, Huzhou, China
[d] State Key Laboratory of Crop Stress Biology for Arid Areas, Northwest A&F University, Yangling, Shaanxi, China

## ARTICLE INFO

## ABSTRACT

The silkworm, *Bombyx mori*, is utilized as a research model in many aspects of biological studies, including genetics, development and immunology. Previous biochemical and genomic studies have elucidated the silkworm immunity in response to infections elicited by bacteria, fungi, microsporidia, and viruses. The intestine serves as the front line in the battle between insects and ingested harmful microorganisms. In this study, we performed RNA sequencing (RNA-seq) of the larval silkworm midgut after oral infection with the Gram-positive bacterium *Bacillus bombysepticus* and the Gram-negative bacterium *Yersinia pseudotuberculosis*. This enables us to get a comprehensive understanding of the midgut responses to bacterial infection. We found that *B. bombysepticus* induced much stronger immune responses than *Y. pseudotuberculosis* did. Bacterial infection resulted in more energy consumption including carbohydrates and fatty acids. The midgut immune system was characterized by the generation of reactive oxygen species and antimicrobial peptides. The former played a critical role in eliminating invading bacteria during early stage, while the latter executed during late stage. Our results provide an integrated insight into the midgut systematic responses to bacterial infection.

## 1. Introduction

As a truly domesticated insect, the silkworm, *Bombyx mori*, has been associated with human for a long time (Goldsmith et al., 2005). Sericulture is a traditional agricultural industry and of economic importance in East and Southeast Asia. The silkworm was also considered as a model for scientific research in many aspects of biology (Goldsmith et al., 2005; Xia et al., 2014). Scientists used the silkworm to decipher the interactions between insect and bacteria or fungi (Chen and Lu, 2018; Ishii et al., 2015; Kaito, 2016).

When the silkworm encounters microorganisms, it mounts a variety of responses to defend itself against the invasion and infection of the microorganisms. In the first step, the silkworm recognition proteins interact with pathogen associated molecular pattern (PAMP) (e.g., lipopolysaccharide, peptidoglycan, β-1, 3-glucan) associated with microbes and trigger host immune responses (Koizumi et al., 1999; Shu

et al., 2016; Zhang et al., 2014). These include hemocytes-mediated reactions (Koizumi et al., 1999; Shu et al., 2016; Zhang et al., 2014), phenoloxidase catalyzed melanization (Chen et al., 2016; J. Li et al., 2016; Ochiai and Ashida, 1988; Yoshida et al., 1996), reactive oxygen species (ROS), and induction of antimicrobial peptides (AMPs) (Cheng et al., 2006; Chowdhury et al., 1995; Furukawa et al., 1999; Hara and Yamakawa, 1995; Kato et al., 1993; Kaneko et al., 2007; Yang et al., 1999, 2011). Insect AMP genes are regulated by the Toll and IMD (immune deficiency) pathway via nuclear factor-κB (NF-κB) factors (Dorsal and Relish). The Toll pathway was mainly activated by the endogenous ligand Spätzle (SPZ), and cascaded downstream signaling from adaptor molecules MyD88, and the kinase Tube, Pelle, to the inhibitor of NF-κB (Cactus). The IMD pathway, including the upstream pattern recognition receptors (PGRP-LC and PGRP-LE) and the downstream signaling molecules (Fadd, Dredd, Tak1/Tab2, IKK), was activated by meso-diaminopimelic acid-type peptidoglycans (Hoffmann

and Reichhart, 2002; Lemaitre and Hoffmann, 2007; Kanost et al., 2004). The silkworm might also regulate hemostasis of nutrients (for instance, iron) to microorganisms and block their growth as a defense strategy (Otho et al., 2016). Genome wide surveys were performed in the last several years in order to provide scenarios of responses of the silkworm to infections by bacteria, fungi, microsporidia and viruses (Cheng et al., 2016; Hou et al., 2014; Huang et al., 2009; Jiang et al., 2016; Kolliopoulou et al., 2015; Ma et al., 2013; Tanaka et al., 2008; Wang et al., 2015; Yue et al., 2015).

As a matter of fact, digestion tract is the front line of the combat between insects and ingested microorganisms. Using the fruit fly, *Drosophila melanogaster*, as a model, it has been established that productions of AMPs and ROS are the principal mechanisms in the gut to eliminate pathogenic bacteria (Buchon et al., 2013). Immune response and metabolic regulation are inseparable. In *D. melanogaster*, transcription factor MEF2, ROS production and extracellular adenosine were directly or indirectly as a critical switch between anabolic and immune function (Bajgar et al., 2015; Clark et al., 2013; Masuzzo and Royet, 2018). In the silkworm, many evidences indicate that both AMPs and ROS play roles in defense of ingested microorganisms in concert (Hu et al., 2013, 2015; Wang et al., 2016; Wu et al., 2010b; Zhang and Lu, 2015; Zhang et al., 2015). Genome wide studies that investigated molecular mechanisms of the interaction between pathogens and silkworm were already reported in the past (X.S. Li et al., 2016; Xu et al., 2012). However, the immune response of midgut that is the first barrier after orally infection is still unclear. In order to get a comprehensive view of systemic responses of midgut against bacterial infection, we carried out RNA sequencing (RNA-seq) analysis of the silkworm gut infected with different bacteria and further investigations to explore the immune mechanism.

## 2. Experimental section

### 2.1. Silkworm and bacteria

Silkworm (*Nistari*) eggs larvae were reared on fresh mulberry leaves at $27 \pm 1$ °C, photoperiod 14L:10D, and $65 \pm 10\%$ relative humidity (Chen et al., 2014). *Y. pseudotuberculosis* and *B. bombyseptieus* were cultured overnight in 30 mL Luria-Bertani medium (1% tryptone, 0.5% yeast extract, 0.5% NaCl in w/v) at 37 °C, then were harvested from cultures by centrifugation at 5000 *g* for 5 min, washed three times with sterile 0.85% NaCl solution, and resuspended to the required concentrations with 0.85% NaCl solution. Freshly prepared bacterial suspensions were used for all experiments.

### 2.2. Oral infection and survival analysis

The indigenous bacteria were eliminated by 5 μL (10 μg/μL) tetracycline coated on mulberry leaves (5 mm × 5 mm) for each 5th instar, day 2 larva. The larvae were used for oral infection after 24 h. Briefly, bacterial suspensions were coated on pieces of mulberry leave and were fed to the tested larvae. Only the larvae finished their feeding in 30 min were used for the next assays. To record the survival rates of silkworm larvae after feeding with bacteria, twenty silkworm larvae in each group were respectively challenged with $1 \times 10^6$, $1 \times 10^7$, $1 \times 10^8$, or $1 \times 10^9$ cells of *Y. pseudotuberculosis*, *B. bombyseptieus*, or 0.85% NaCl (control) by feeding. The number of dead silkworms was recorded, and the survival curves of silkworms with different treatment were compared using log-rank test by Graphpad Prism5 (GraphPad Software, Inc., La Jolla, CA, USA).

### 2.3. RNA extraction and cDNA preparation

The samples of midgut were collected from silkworms infected with $1 \times 10^8$ cells of *Y. pseudotuberculosis*, *B. bombyseptieus* or 0.85% NaCl (control) by feeding at 4 and 48 h post-injection. Three replicates for each treatment described below were performed on different dates to provide biological replication. Samples of midgut were homogenized and lysed in Tripure RNA Isolation Reagent (Roche, Basel, Switzerland). Total RNA was extracted according to the protocol (Roche, Basel, Switzerland). RNA concentrations were determined on a Nanodrop ND-2000 spectrophotometer (NanoDrop products, USA). RNA integrity was verified on an Agilent 2100 BioAnalyzer (Agilent, Palo Alto, USA). For each reaction, 1 μg total RNA was treated with DNase I (Invitrogen, Carlsbad, USA) to remove genomic DNA. cDNA syntheses were constructed using an Maloney murine leukemia virus (M-MLV) reverse transcriptase kit according to the protocol (Promega, Madison, USA).

### 2.4. Library construction and sequencing

As described previously (Xiong et al., 2015), 10 μg of total RNA from each treatment or control group was used to enrich poly(A) mRNA using oligo(dT) magnetic beads (Invitrogen, Carlsbad, USA). The paired-end RNA-seq libraries were constructed by following the Illumina's library construction protocol, and sequenced on Illumina HiSeq™ 4000 platform (Illumina, San Diego, USA). FASTQ files of raw-reads were produced and sorted out by barcodes for further analysis.

### 2.5. Assembly and annotation of transcriptomes

After removal of adaptor sequences, low quality, and contaminated reads, only the resulting clean reads were assembled to build contigs using Trinity, the short reads assembling program version 2013 (Grabherr et al., 2011). The assembled transcript sets were pooled for clustering using CD-hit software (version 4.5.4) (Li and Godzik, 2006), and were manually refined to generate the final unigene version.

For functional annotations, Blast2GO was used to annotate genes from the Trinity transcripts. All the assembled sequences were annotated against the NCBI non-redundant (NR) protein sequences database using BLASTX (E-value $\leq 1e^{-5}$) as we described previously (Xiong et al., 2015). In addition, possible gene functions were assessed based on analysis using Gene Ontology (GO) (Ashburner et al., 2000). Pathway annotation was assigned to the KEGG Orthology Based Annotation System (KOBAS) online service (http://kobas.cbi.pku.edu.cn/home.do) (Wu et al., 2006; Xie et al., 2011).

### 2.6. Analysis of differentially expressed transcripts

Transcripts of the control and treated samples were mapped, based on expression profile comparisons. Clean reads of each library were mapped to the unigenes using Bowtie software (http://bowtie-bio.sourceforge.net/index.shtml) with the default parameters. RSEM, the utility package of the Trinity software was performed to calculation of normalized gene expression value FPKM (fragments per kilobase per million mapped reads). Differentially expressed transcripts (DETs) were calculated using DEGseq package in R environment (P-value < 0.001, fold change > 2) (Wang et al., 2010).

### 2.7. Quantitative real-time PCR analysis

The quantitative real-time RT-PCR (qRT-PCR) reactions for all samples were performed on the Rotor-geneQ system (Qiagen, Dusseldorf, Germany) and reaction system was prepared according to the protocol provided with 2 × FastStart Essential DNA Green Master (Roche, Basel, Switzerland). All primers used in real-time are designed by Primer5 and presented in Additional file 1: Table S1. Thermal cycling conditions were: initial denaturation at 95 °C for 10 min, followed by 40 cycles of denaturation at 95 °C for 20 s, annealing at 53 °C for 20 s and extension at 72 °C for 20 s. A melting curve (60–95 °C) was determined to confirm amplification of the desired PCR products. All reactions were carried out in quadruplicate. IF4A (DQ443290.1) was used an internal standard to normalize the templates. qRT-PCR data were

collected and preliminary analyzed with the Rotro-geneQ software, then exported to EXCEL for ulterior analysis. The relative mRNA abundance were calculated by $2^{-\Delta\Delta CT}$ method which $\Delta\Delta CT = (CT_{target} - CT_{reference})_{treated} - (CT_{target} - CT_{reference})_{control}$. Figures were drawn using software Graphpad. The data were analyzed using the Student's *t*-test. Asterisks indicate significant differences: *p < 0.05; **p < 0.01; ***p < 0.001.

### 2.8. Hydrogen peroxide and nitric oxide assay

Five silkworm larvae infected with $1 \times 10^8$ cells of bacteria or 0.85% NaCl solution by feeding were dissected to collect peritrophic membranes with contents (PMC) at 4 h, 24 h and 48 h. The PMC was centrifuged at 13,000 g and 4 °C for 5 min, and then the supernatants from the gut contents were transferred to Amicon Ultra 10 K filters (Millipore, Billerica, MA, USA) and centrifuged at 13,000 g and 4 °C for 5 min $H_2O_2$ concentrations in the flow-through samples from the Amicon Ultra 10 K filters were measured using an Amplex Red Hydrogen Peroxide/Peroxidase Assay kit (Invitrogen, Carlsbad, CA, USA) (Zhang and Lu, 2015). Meanwhile, the concentration of nitric oxide was determined using Total Nitric Oxide Assay Kit (Beyotime, Beijing, China) according to the manufacturer's instructions.

### 2.9. Bacteria number counting and antibacterial activity assay

Three silkworm larvae infected with $1 \times 10^8$ cells of bacteria or 0.85% NaCl solution by feeding were dissected to collect peritrophic membranes with contents (PMC) at 4 h, 24 h and 48 h. To detect the change of bacterial number in the silkworm gut, PMC was weighted and mixed well. The mixture was mixed well with 40 vol of LB medium in a 50 mL tube, and then placed the tube on a tube holder for 2 min at room temperature, then 10 μL supernatants were spread in LB agar plate. The colony forming units (CFUs) were calculated in LB agar plate after cultured overnight.

To assay the antibacterial activity of gut content, the digestion juice were separated from PMC by centrifugation at 13,000 g and 4 °C for 10 min. The digestion juice were incubated at 100 °C for 5min and then centrifuged at 13,000 g and 4 °C for 10 min. 4 μL supernatant from the group infected by *B. bombyseptieus* or *Y. pseudotuberculosis* was loaded to the wells in the LB agar plates containing *B. bombyseptieus* or *Y. pseudotuberculosis*, respectively. The group fed with 0.85% NaCl solution was used as control group. The antimicrobial activity assay was performed by measuring zones of growth inhibition in a thin layer of agar plates, as described previously (Hoffmann et al., 1981).

## 3. Results

### 3.1. Survival of the silkworm larvae after oral infection with Y. pseudotuberculosis and B. Bombyseptieus

In order to investigate the responses against ingested bacteria, we fed the silkworm larvae with *Y. pseudotuberculosis* (Gram-negative bacterium) and *B. bombyseptieus* (Gram-positive bacterium). Two days after infection, *B. bombyseptieus* caused more larvae mortality than *Y. pseudotuberculosis* (Fig. 1), indicating that larval silkworms were more susceptible to *B. bombyseptieus* at the early stage of infection. However, in the late stage, larvae were more susceptible to *Y. pseudotuberculosis* than to *B. bombyseptieus*. A certain concentration of bacteria can active the immunity, but it may not cause the high mortality. In the following experiments, we used $1 \times 10^8$ cells of bacteria in oral infection experiment.

### 3.2. Characterization of silkworm midgut transcriptome by illumina RNA sequencing

Midguts were collected from *Y. pseudotuberculosis* and *B.*

*bombyseptieus* infected silkworm larvae at 4 h (early stage) and 48 h (late stage) post infection. In total, eighteen RNA samples (three biological replications) were used for constructing cDNA libraries. These libraries were sequenced on an Illumina HiSeq™ 4000 sequencer. After removing adaptor sequences and low-quality reads (Q < 20), it yielded 42.2 (C4_1), 35.9 (C4_2), 41.9 (C4_3), 32.2 (B4_1), 40.5 (B4_2), 44.2 (B4_3), 40.9 (Y4_1), 41.1 (Y4_2), 37.6 (Y4_3) 43.7 (C48_1), 39.7 (C48_2), 50.1 (C48_3), 46.6 (B48_1), 38.7 (B48_2), 37.2 (B48_3), 34.9 (Y48_1), 44.8 (Y48_2), 28.1 (Y48_3) million high quality reads (Additional file 2: Table S2). The correlation coefficient of biological replicated samples calculated using the Pearson correlation module in R were more than 80% (Additional file 3: Table S3). Then, pooled clean reads from these eighteen libraries were de novo assembled using the Trinity software and produced 65,822 unigenes (Additional file 4: Table S4) with mean lengths of 791 nt and total bases of 52,093,116 nt and N50 length of 1568 nt (Additional file 5: Table S5). In the end, unigenes were annotated using Blast2GO against the GenBank non-redundant database, and 17,593 unigenes with homologous to the known proteins were obtained (E-value < 1e-5) (Additional file 6: Table S6).

To observe transcriptional changes in the infected midgut, differentially expressed transcripts (DETs) were identified after pairwise comparisons between infected and control group (Wang et al., 2010). 3948 transcripts in the bacterial infection groups with *P*-value < 0.05 and fold change > 2 were identified as differently expressed transcripts. The identified DETs with FPKM (fragments per kilobase of transcript per million) values were presented in Additional file 7: Table S7.

To reveal the difference of midgut responses between *B. bombyseptieus* infected and *Y. pseudotuberculosis* infected group, hierarchical clustering of DETs revealed four clusters (Fig. 2A). Most of DETs in the cluster 1 and 2 had the higher mRNA levels at 4 hpi, and then were significantly down-regulated at 48 hpi. In the cluster 3 and 4, DETs had low mRNA levels or were suppressed at 4 hpi, but there were a remarkable increase of mRNA levels at 48 hpi, especially in Y48 group (Fig. 2A). Venn diagram analysis enable us to identify transcripts specifically regulated by *B. bombyseptieus* (1034 down-regulated and 1095 up-regulated at 4 hpi, 146 down-regulated and 187 up-regulated at 48 hpi, respectively) and *Y. pseudotuberculosis* (131 down-regulated and 222 up-regulated at 4 hpi, 393 down-regulated and 448 up-regulated at 48 hpi, respectively). The number of DETs regulated by *B. bombyseptieus* (2789) is about 2.75 folds than that of DETs regulated by *Y. pseudotuberculosis* (1013) at 4 hpi, but *B. bombyseptieus* infected group (706) is 1.72 folds lower than *Y. pseudotuberculosis* infected group (1214) at 48 hpi. Many transcripts (5 transcripts at 4 hpi, 12 transcripts at 48 hpi) were up-regulated by *Y. pseudotuberculosis* but down-regulated by *B. bombyseptieus* (Fig. 2B). These results were consistent with those revealed by hierarchical clustering that the transcriptomes of midgut of silkworm infected by those bacteria were regulated differently.

Comparative analysis of Gene Ontology (GO) enrichment (Ashburner et al., 2000) indicated that GO terms enriched (p-value < 0.05) between *B. bombyseptieus* and *Y. pseudotuberculosis* infections at 4 and 48 hpi were 27 and 20 respectively, which showed gradual decrease with the infection time prolongation (Fig. 3A). The GO terms enriched in *B. bombyseptieus* infected group were significantly more than *Y. pseudotuberculosis* infected group at 4 hpi (Fig. 3A). On the contrary, the GO terms enriched in *Y. pseudotuberculosis* infected group were significantly more than *B. bombyseptieus* infected group at 48 hpi (Fig. 3A). These results suggest the Gram-positive bacteria might induce stronger responses than *Y. pseudotuberculosis*.

KEGG pathway analysis (Wu et al., 2006; Xie et al., 2011) reveal that some metabolic pathways of silkworms infected by *B. bombyseptieus* and *Y. pseudotuberculosis* was significantly enriched, suggesting the bacterial invasion is able to result in more energy consumption to eliminate the invading microbes (Fig. 3B). Translation pathway was enriched in groups infected at 4 h by B. *bombyseptieus* and *Y. pseudotuberculosis*, indicating that protein level in the midgut of silkworms was up-regulated in response to bacterial infection in early stage (Fig. 3B).
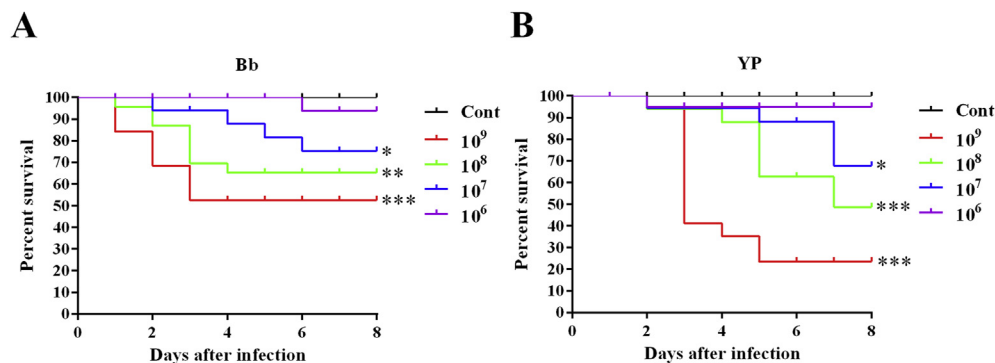
**Fig. 1.** Survival of silkworm larvae after fed with different doses of bacteria. The silkworm larvae were fed with mulberry leaves containing different doses of *B. bombyseptieus* **(A)** and *Y. pseudotuberculosis* **(B)**. The silkworm larvae in the control group were fed with 0.85% NaCl solution. Twenty larvae were included in each group. Cont, control group; YP, *Y. pseudotuberculosis* infected group; Bb, *B. bombyseptieus* infected group. Asterisks indicate significant differences: *$p < 0.05$; **$p < 0.01$; ***$p < 0.001$ for pairwise comparisons by log-rank test.

The pathway of infection diseases: Bacteria was enriched in *B. bombyseptieus* infected groups at 4 h, but enriched in *Y. pseudotuberculosis* infected groups at 48 h (Fig. 3B). Those results clearly indicate that the transcriptome of silkworm was regulated after bacterial infection in different periods. It indicates that the difference between the times after infection was much more significant than that between different pathogens.

Taken together, our results suggested that expression profiling of genes in the midgut highly depends on the infection time and the way of treatments. In most animals' gut, there harbor many bacteria (Dillon and Dillon, 2004; Ley et al., 2008). During the process of evolution, insects construct an efficient defending system to keep the balance between the host immune responses and pathogenic bacteria for gut microbial homeostasis (Artis, 2008; Sansonetti, 2004). For further analysis of the interactions between silkworm midgut and pathogens, we identified 58 differential expressed immunity-related genes (Additional file 8: Table S8), and re-examined their mRNA expression levels of genes, which are regulated by *B. bombyseptieus* and *Y. pseudotuberculosis*.

### 3.3. Expression profile of metabolism related genes in the silkworm midgut in response to bacterial challenge

Metabolic regulation is closely linked with immune responses (Hotamisligil, 2006). In *D. melanogaster*, chronic or acute infection disrupts metabolism processes (Lee and Lee, 2018). The immune response is energetically costly through activating corresponding physiological responses in insects (Ardia et al., 2012; Freitak et al., 2003). The pathway of carbohydrate metabolism, including glycolysis TCA (tricarboxylic acid cycle) and PPP (pentose phosphate pathway), directly generates ATP (adenosine triphosphate). However, fat acid is catabolized through a series of enzyme-catalyzed reactions converting to dihydroxyacetone phosphate, a glycolytic intermediate. The KEGG pathway analysis showed that abundant genes were mapped on processing in carbohydrate and lipid metabolism (Fig. 3B). Most carbohydrate metabolic genes had the higher mRNA levels at 4 hpi, suggesting the carbohydrate metabolic pathway is activated at early infection stage (Fig. 4A, Additional files 9:Table S9). The key enzymes in glycolysis (*phosphofructokinase, hexokinase and phosphofructokinase*) and TCA (*isocitrate dehydrogenase*) expression were further confirmed by qRT-PCR, and mRNA abundance of these enzymes increased at 4 hpi. Fat acid metabolic genes, particularly *lipases*, had the higher mRNA levels at 48 hpi, indicating that fat acid metabolic response in the late stage after bacterial challenge (Fig. 4B, Additional files 9: Table S9). These results suggest that bacterial invasion not only activates the immune pathways, but affects the metabolic pathways also.

### 3.4. Immune responses to bacterial infections in the silkworm midgut

Insects rely on immune system to eliminate invading pathogens for survival (Akira et al., 2006; Hoffmann and Reichhart, 2002; Kanost et al., 2004). The *D. melanogaster* intestinal immune system produces ROS and AMPs to defend itself against ingested pathogens (Charroux and Royet, 2012; Fang, 2004; Ryu et al., 2010). IMD and JAK-STAT
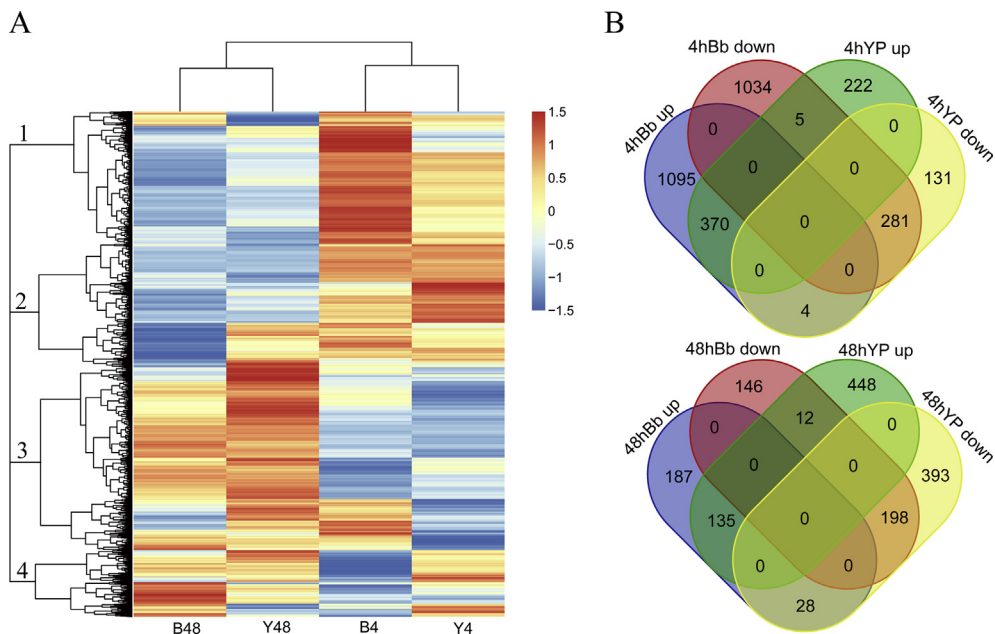


**Fig. 2.** Hierarchical clustering analysis and venn diagram of DETs in midgut of silkworm larvae infected by *Y. pseudotuberculosis* and *B. bombyseptieus*. **(A)** Hierarchical clustering analysis of all the DETs (the fold change is significantly more than 2, $p < 0.001$) in midgut of silkworm larvae infected by *B. bombyseptieus* and *Y. pseudotuberculosis*. The heatmap is divided into four discrete clusters. **(B)** Venn diagram of differentially expressed transcripts in midgut of silkworm larvae infected by *B. bombyseptieus* and *Y. pseudotuberculosis*. Numbers of up-regulated and down-regulated transcripts were indicated. All the FPKM values of infected group were normlized based on corresponding the FPKM values of conrol group. YP or Y, *Y. pseudotuberculosis* infected group; Bb or B, *B. bombyseptieus* infected group; 4, 4 h post infection; 48, 48 h post infection.

A
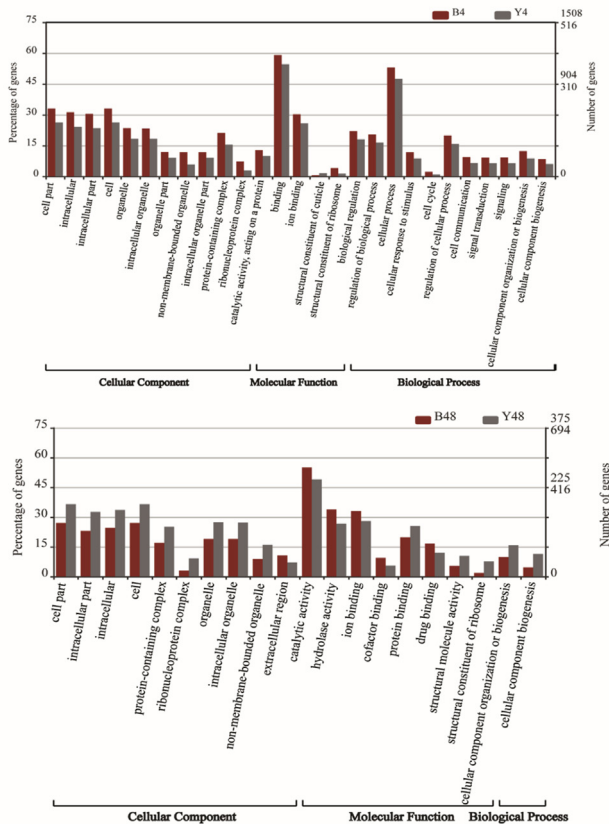


B
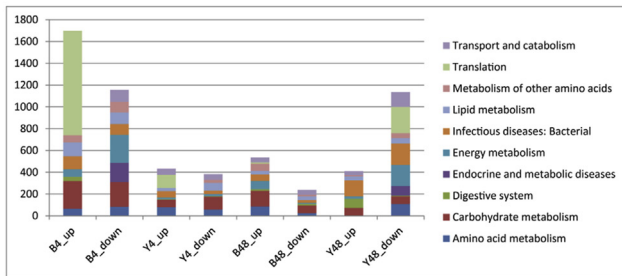


**Fig. 3.** Comparative transcripome analysis in midgut of silkworm larvae infected with *B. bombyseptieus* and *Y. pseudotuberculosis*. **(A)** Gene ontology (GO) annotation of DETs in the silkworm midgut transcriptome. Enriched GO analysis (* for p < 0.05) of DETs between *B. bombyseptieus* (Red) and *Y. pseudotuberculosis* (Grey) infection are performed by pairwise comparison with the corresponding control group of 4 h (upper panel) and 48 h (lower panel). Level 2 GO assignments are made in terms of cellular components, molecular functions, and biological processes. **(B)** Distribution of KEGG functional groups within up- and down-regulated gene cohorts in midgut from the *B. bombyseptieus* and *Y. pseudotuberculosis* infected larvae. The bar chart corresponds to the matched entries of DETs in their own functional category. Y, *Y. pseudotuberculosis* infected group; B, *B. bombyseptieus* infected group, 4, 4 h post infection; 48, 48 h post infection. (For interpretation of the references to colour in this figure legend, the reader is referred to the Web version of this article.)

(Janus Kinases-Signal Transducers and Activators of Transcription), but not Toll pathway, construct the second line of defense against ROS resistant bacteria in *D. melanogaster* gut (Buchon et al., 2009; Ryu et al., 2006). In silkworm gut, there are several studies implying that Toll, JAK/STAT and IMD pathways are synergistically involved in the immune response (Wu et al., 2010a, 2010b). It seems that the immune signaling pathways of silkworm gut are different from those of *D. melanogaster* gut. Therefore, more data is needed to confirm the Toll

pathway in silkworm gut.

In our study, 58 immunity-related genes were identified to significantly expressed in midgut transcriptome (Additional files 8:Table S8). Genes involved in immune recognition were up-regulated by *B. bombyseptieus* and *Y. pseudotuberculosis* (Fig. 5A). Similarly, Toll, IMD, JNK and JAK/STAT pathway genes were induced, suggesting that they are involved in the immune response (Fig. 5B). Hierarchical clustering revealed that AMP genes expression were significantly up-regulated at early and late stage of infection (Fig. 5D), while ROS metabolism genes (e.g., *NOS1*) were up-regulated at early stage of infection (Fig. 5C).

To verify the FPKM value, we used qRT-PCR to examine 14 immunity-related genes expression, and found that the qRT-PCR results were consistent with the RNA-seq data, suggesting that RNA-seq data were reliable. It also indicated that ROS related genes, *NOS1* and *SOD1*, were up-regulated at 4 hpi but tended to the corresponding control groups at 48 hpi, and the transcription of *Prx1* that is able to degrade excess $H_2O_2$ was up-regulated at 4 hpi (Fig. 5C). Pathogen recognition proteins (*PGRP-S2, PGRP-S5, βGRP1*) had higher mRNA levels at 4 hpi, indicating that recognized molecules were activated at the early stage. Expression of the genes involved in the pathways of Toll (*cactus*), IMD (*Iap2* and *Relish*), JNK (*Jun*) and JAK/STAT (*Domeless* and *SOCS*) and other immunity-related genes (*caspase3*) were confirmed by qRT-PCR, suggesting that several pathways play roles in silkworm midgut immune system (Fig. 5B). Effector genes (*Gloverin2, CecB6, Attacin* and *Lys*) were up-regulated after infection, indicating that the larval silkworm produces more AMPs in its gut to eliminate invading bacteria.

*3.5. ROS plays important roles in eliminating invading bacteria at early stage in silkworm midgut*

ROS plays an important role in eliminating invading pathogens, but excess ROS are harmful to the host (Jones et al., 2013; Krause, 2007; Kumar et al., 2010). Hydrogen peroxide and nitric oxide are two kinds of ROS. Hydrogen peroxide is mainly catalyzed by Duox (dual oxidase) and NOX (NADPH oxidoreductase), and nitric oxide is catalyzed by NOS (Nitric Oxide Synthase) (Eleftherianos et al., 2009; Fang, 2004; Lemaitre and Hoffmann, 2007; Knowles and Moncada, 1994). Catalase is a protective enzyme responsible for the degradation of excess hydrogen peroxide and involved in maintaining ROS homeostasis in insects (Switala and Loewen, 2002). To verify the transcriptome data and the qRT-PCR results of ROS related genes, the concentrations of hydrogen peroxide and nitric oxide in the silkworm gut after bacterial infections were determined (Fig. 6). The concentrations of hydrogen peroxide and nitric oxide increased from 4 h to 24 h post infection, which is consistent with the expressions of *SOD1* and *NOS1* (Fig. 5C), and then decreased from 24 h to 48 h because the expression of *Prx1* was up-regulated (Figs. 5C and 6A and B). This suggests that ROS is required at early stage after bacterial infection for silkworm to eliminate ingested bacteria in the gut.

*3.6. Bacterial growth and antimicrobial activity in the silkworm gut after infection*

Compared to ROS, AMPs are produced at the late stage after bacterial infection, but provide a powerful defense against pathogenic bacteria, fungi and parasites (Bulet et al., 1999; Hultmark, 2003; Li et al., 2012). *B. bombyseptieus* belongs to the genus of *Bacillus* that is a pathogen to silkworm and produces spores and parasporal crystals (Huang et al., 2009). In response to severe conditions, *Y. pseudotuberculosis* is able to form biofilm which makes the bacteria more resistant to antibiotics, chlorine, and host immune system (Drenkard and Ausubel, 2002; Joshua et al., 2003; Singh et al., 2002). To examine these two bacteria in the silkworm gut, bacteria number in each group was counted, and we found that the bacteria in both *B. bombyseptieus* and *Y. pseudotuberculosis* infected groups increased from 4 h to 24 h, and then decreased from 24 h to 48 h, but *Y. pseudotuberculosis*
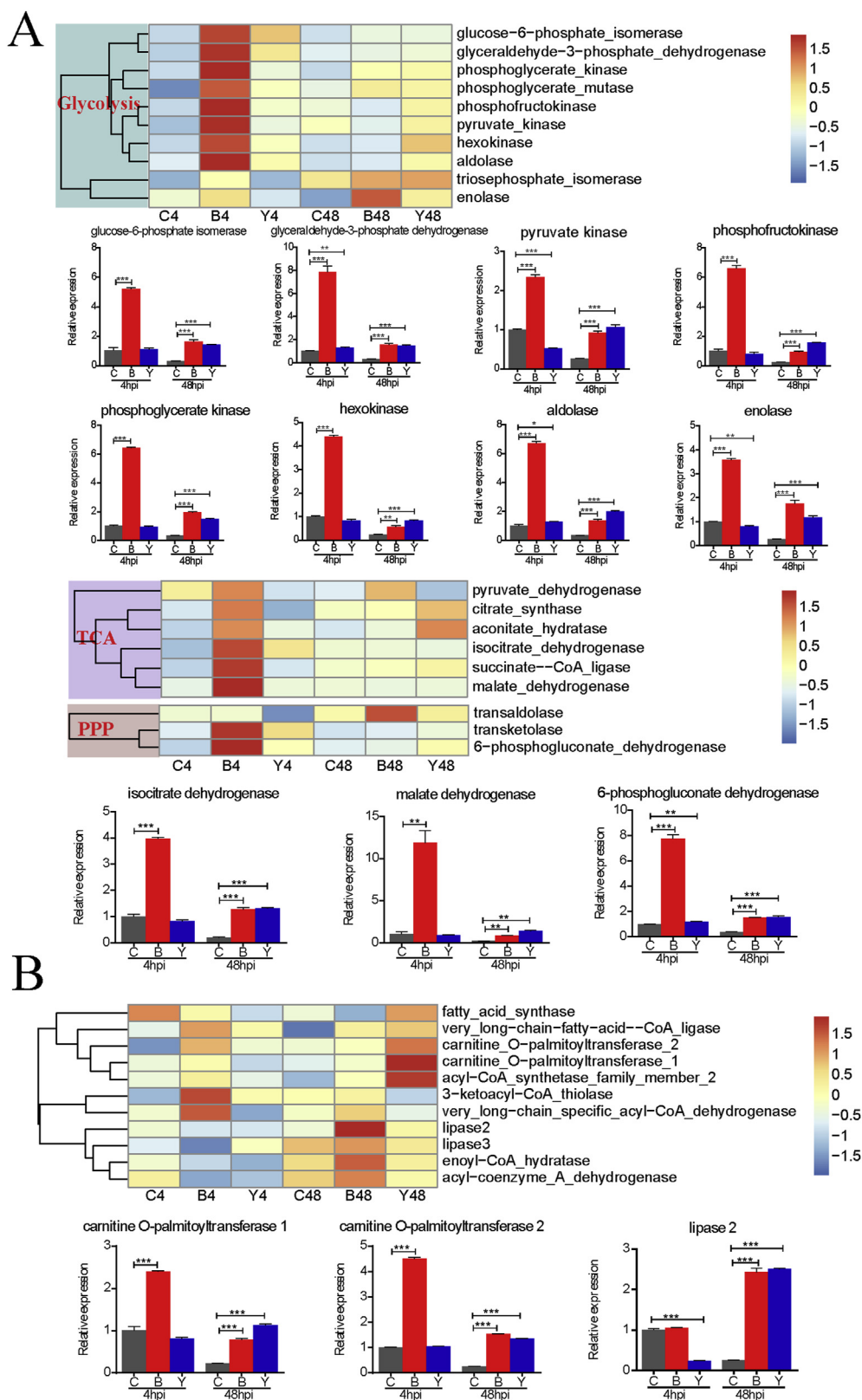
**Fig. 4.** Expression patterns of midgut metabolism-related genes in silkworm midgut. **(A)** Hierarchical clustering analysis and qRT-PCR analysis of carbohydrate metabolism-related genes in the silkworm midgut. **(B)** Hierarchical clustering analysis and qRT-PCR analysis of fatty acid metabolism-related genes in the silkworm midgut. TCA: tricarboxylic acid cycle, PPP: pentose phosphate pathway, C: control group; B, *B. bombyseptieus* infected group; Y, *Y. pseudotuberculosis* infected group; 4, 4 h post infection; 48, 48 h post infection. Asterisks indicate significant differences: *p < 0.05; **p < 0.01; ***p < 0.001 for pairwise comparisons by Student's *t*-test.
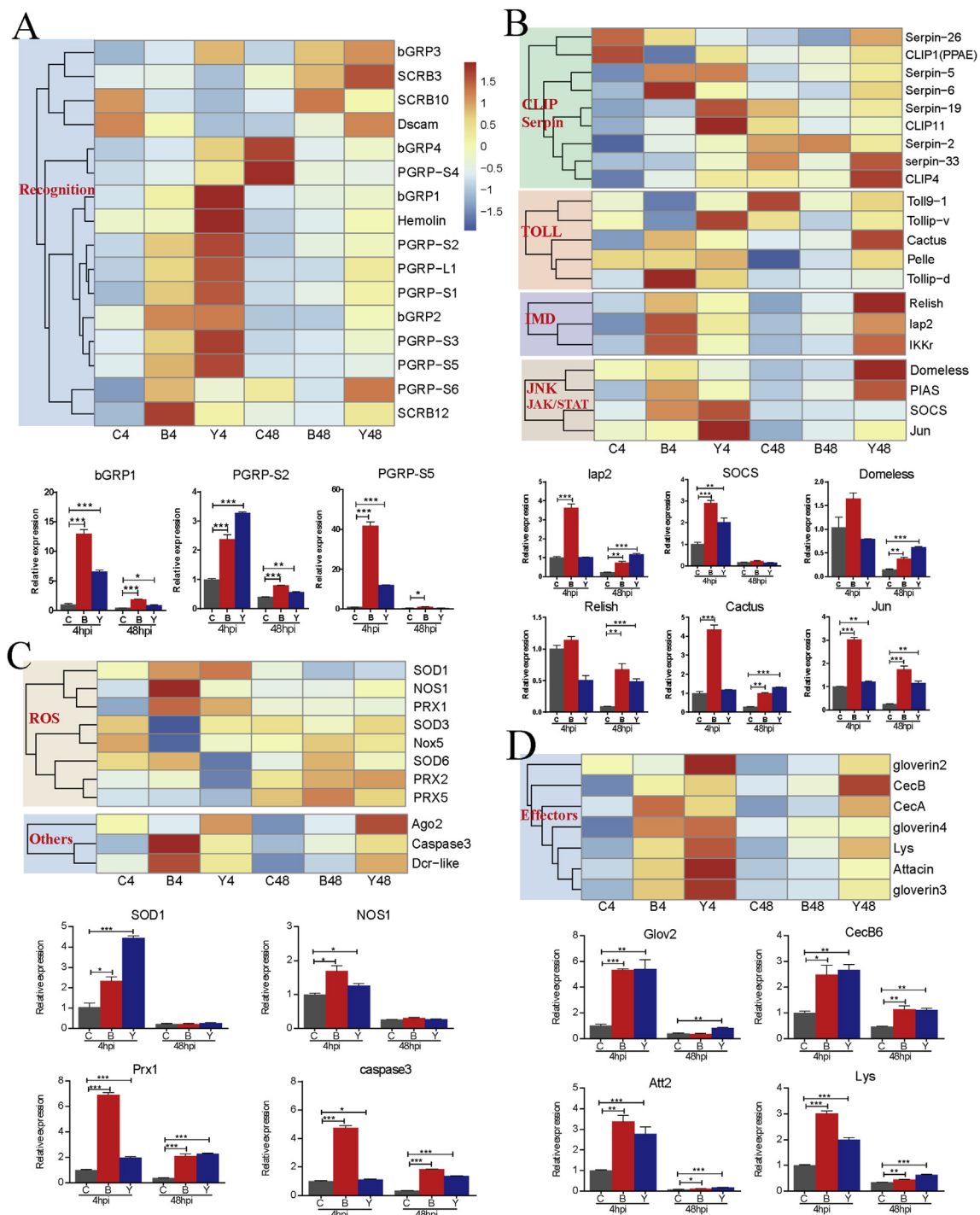
**Fig. 5.** Expression patterns of midgut immunity-related genes in silkworm. **(A)** Hierarchical clustering analysis and qRT-PCR analysis of immune recognition related genes. **(B)** Hierarchical clustering analysis and qRT-PCR analysis of immune regulator related genes. **(C)** Hierarchical clustering analysis and qRT-PCR analysis of ROS-related genes and other immune molecules in the silkworm midgut. **(D)** Hierarchical clustering analysis and qRT-PCR analysis of immune effector related genes in the silkworm midgut. C, control group; B, *B. bombyseptieus* infected group; Y, *Y. pseudotuberculosis* infected group; 4, 4 h post infection; 24, 24 h post infection; 48, 48 h post infection. Asterisks indicate significant differences: *p < 0.05; **p < 0.01; ***p < 0.001 for pairwise comparisons by Student's *t*-test.

reproduced at 72 hpi (Fig. 7A and B). The high concentrations of hydrogen peroxide and nitric oxide in the silkworm gut at 24 hpi could kill bacteria, leading to the reduction of bacteria number after 24 hpi (Fig. 6A and B). In addition, the antimicrobial activity of digestion juice in the silkworm gut was measured (Fig. 7C and D). Compared to the control groups, the antimicrobial activity of infected group did not changed significantly at 4 h post infection, but the activity of infected group significantly increased at 24 h and 48 h post infection, especially

at 48 h post infection (Fig. 7C and D). The transcriptional expression of *AMPs* were up-regulated from 4 h to 48 h after bacterial challenge in transcript level, implying the AMPs accumulated to a certain amount can kill bacteria. Those results suggest AMPs are responsible for killing bacteria at the late stage of bacterial infection in the silkworm gut.
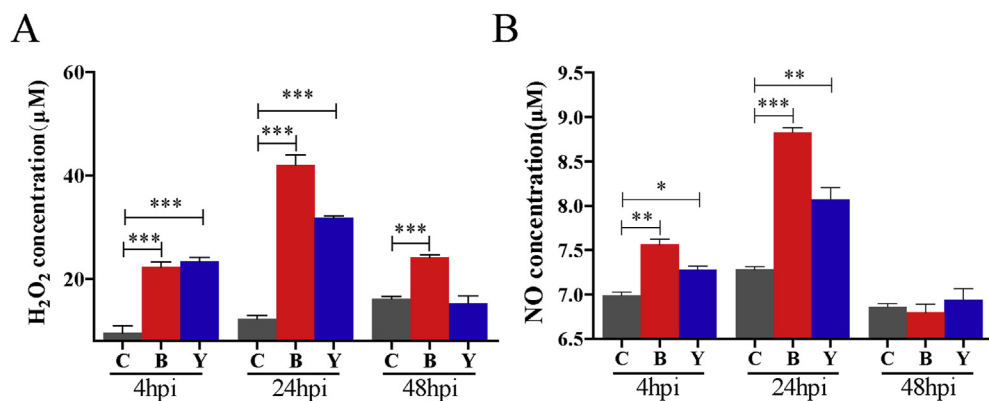
**Fig. 6.** Concentration change of hydrogen peroxide and nitric oxide in silkworm midgut after bacterial infection. **(A)** Concentration of hydrogen peroxide in the silkworm midgut was determined after bacterial infection. **(B)** Concentration of nitric oxide in the silkworm midgut was determined after bacterial infection. C, control group; Y, *Y. pseudotuberculosis* infected group; B, *B. bombyseptieus* infected group; 4, 4 h post infection; 24, 24 h post infection; 48, 48 h post infection. Asterisks indicate significant differences: *$p < 0.05$; **$p < 0.01$; ***$p < 0.001$ for pairwise comparisons by Student's $t$-test.
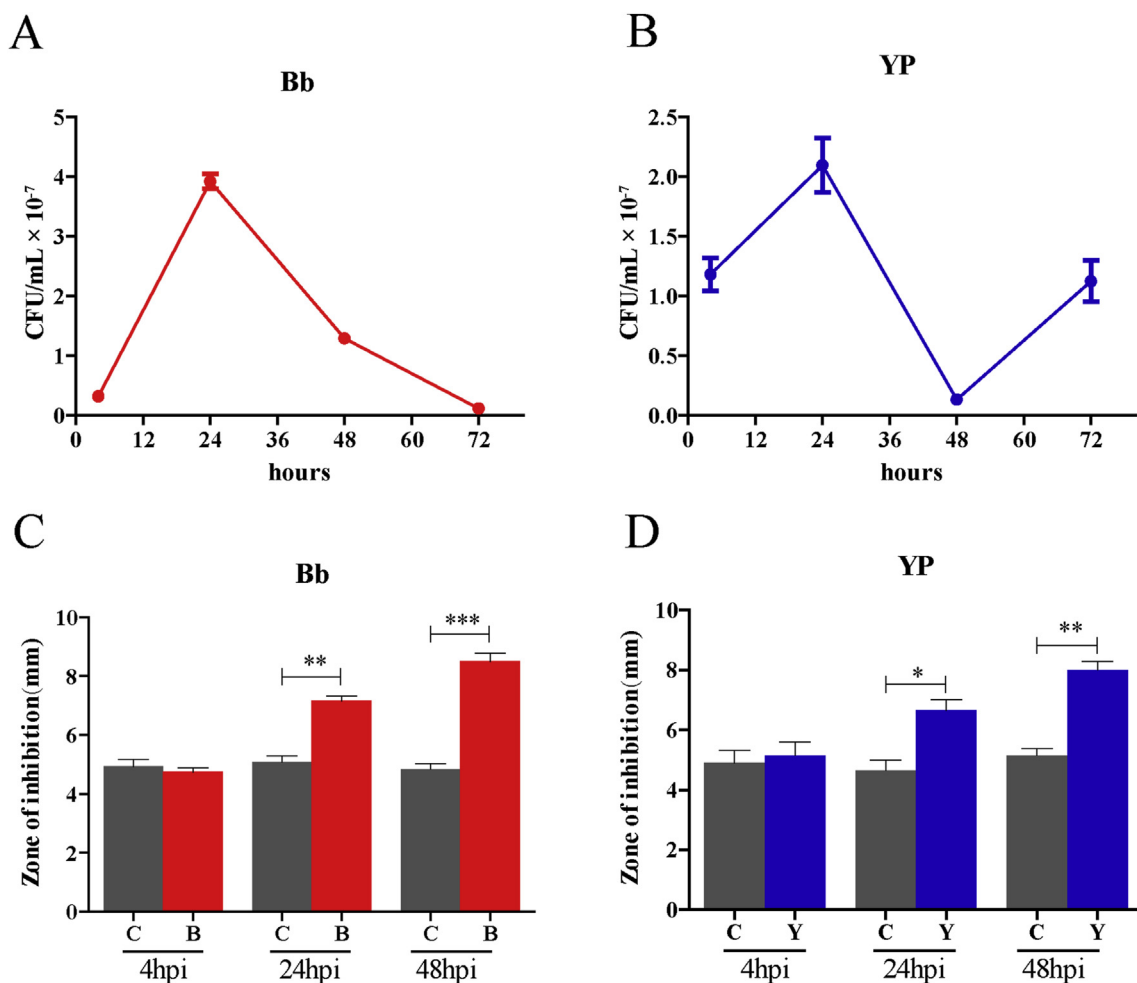


**Fig. 7.** Bacteria number changes and antimicrobial activity in silkworm gut after bacterial infection. The silkworms of infected groups were fed with fresh mulberry leaf containing $1 \times 10^8$ cells of *B. bombyseptieus* **(A)** or *Y. pseudotuberculosis* **(B)**, and then the gut content was collected, diluted and spread on LBB plate to count the CFUs at 4 hpi, 24 hpi, 48 hpi and 72 hpi. After spinning down the bacteria and food residue in the gut content, the supernatant was boiled, and then used for antimicrobial activity assay. The samples from *B. bombyseptieus* and *Y. pseudotuberculosis* were used for antimicrobial activity assay against *B. bombyseptieus* **(C)** and *Y. pseudotuberculosis* **(D)**, respectively. C, control group; Y or YP, *Y. pseudotuberculosis* infected group; B or Bb, *B. bombyseptieus* infected group; 4, 4 h post infection; 24, 24 h post infection; 48, 48 h post infection; 72, 72 h post infection. Asterisks indicate significant differences: *$p < 0.05$; **$p < 0.01$ for pairwise comparisons by Student's $t$-test.

## 4. Discussion

As the first line of response, gut plays a critical role in the interaction of ingested microorganisms and insects. Majority of microorganisms might be cleared by the host's immunity, while rest of them enter into hemocoel through the gut barrier, or they might colonize in the intestine. Here we analyzed the dynamics of global gene expression profiles in the silkworm midgut in response to bacterial infection. Our results demonstrate that the silkworm midgut produces ROS at the early stage and AMPs at the later stage after bacterial infection. In fact, this observation is similar to the previous results obtained in *D. melanogaster* (Buchon et al., 2013). The IMD pathway has been previously reported

to play role in midgut immune responses in insects, such as *B. mori, D. melanogaster, A. gambiae,* and *Rhodnius prolixus* (Dong et al., 2009; Buchon et al., 2013; Ribeiro et al., 2014; Wu et al., 2010b). In *D. melanogaster*, the IMD pathway is crucial in midgut immunity, but the Toll pathway didn't participate in it (Buchon et al., 2013; Tzou et al., 2000; Ryu et al., 2006). However, others studies had revealed that the Toll pathway could be activated in insects, such as *B. mori* and *R. prolixus* (Ribeiro et al., 2014; Wu et al., 2010b). The JAK-STAT pathway could regulate gut epithelium renewal to protecting the gut from ROS and bacterial toxins by the JNK and Hippo pathway (Buchon et al., 2013). Similarly, our data demonstrated the Toll, IMD, JNK, and JAK/STAT pathways were involved in silkworm midgut immunity. However, there are still three questions need to be investigated in the future.

(1) How does the silkworm regulate ROS and AMPs production in its midgut? Production of ROS in the *Drosophila* gut is a quick response, which occurs within a few hours after bacterial infection (Ha et al., 2005a, 2005b). Our results (Figs. 5 and 6) confirmed this in the silkworm midgut. In mosquito *A. aegypti*, it has been found that *Wolbachia* infection induces ROS formation and consequently activates the Toll pathway, which regulates the expression of AMP and antioxidant genes (Pan et al., 2012). ROS was also proven to be involved in the immune response against Dengue virus infection (Wang et al., 2019). In *D. melanogaster*, expression of human paraoxonase, which interferes with ROS in humans and mice, decreases superoxide levels and alters bacterial colonization in the gut (Pezzulo et al., 2012). In mammalian cells, many studies demonstrate that NF-κB is activated by ROS in the early phase (Nakajima and Kitamura, 2013). In our study, the expression of AMP genes and antibacterial activity increased significantly after 24 h post infection (Fig. 7C and D). At this point, whether bacterial infection induced ROS is involved in the regulation of AMP genes expression certainly is not clear. Apart from ROS, we also found that the expression of nitric oxide synthase 1 (*NOS1*) and nitric oxide levels increased 4 h after infection (Figs. 5C and 6B). It has been indicated that nitric oxide regulates AMPs expression in *D. melanogaster* (Foley and O'Farrell, 2003; Nappi et al., 2000). It is worth investigating the role of nitric oxide in insect intestinal defense.

(2) Is the Toll pathway really involved in the silkworm gut immunity? It is clear that the IMD pathway, but not the Toll pathway, plays a fundamental role to mediate AMPs expression in the *D. melanogaster* intestine in response to bacterial infection (Buchon et al., 2013; Tzou et al., 2000; Ryu et al., 200). In silkworm, based on gene expression profile analysis, it suggested that the Toll pathway might be involved in gut immunity along with the IMD and JAK/STAT pathways (Wu et al., 2010b). In this study, we found that several key genes of the Toll pathway, for instance, *Pelle*, *Cactus*, and *Toll9*, were remarkably induced, by bacterial infection (Fig. 5B). Toll and IMD signal pathways could be activated by gram-positive and gram-negative bacteria (Fig. 5B). These results are consistent with some studies. In silkworm, some pattern recognition receptors (PGRP-L1, PGRP-L3, PGRP-S1, PGRP-S2, PGRP-S3, βGRP3, βGRP4) were upregulated by gram-positive and -negative bacteria (Xu et al., 2010; Yang et al., 2017). *Spatzle* (Toll pathway) and *IMD* (IMD pathway) were also activated by gram-positive and -negative bacteria (Wang et al., 2007; Zhan et al., 2018). This observation indicates the Toll pathway might be responsible for AMPs production in silkworm gut. It indicates that silkworm adopt more complicated immune responses. However, genetic and biochemical evidences are definitely needed to confirm this observation.

(3) How do immune response and metabolism response interplay reciprocally in silkworm? In *D. melanogaster*, infection with *Mycobacterium marinum* causes metabolic disruptions, and activation of the Toll pathway in the fly fat body results in metabolic storage (Dionne et al., 2006; DiAngelo et al., 2009). FOXO is able to activate antimicrobial peptide expression but not required for

resistance to infection (Becker et al., 2010). MEF2 through its phosphorylation and dephosphorylation is a critical transcriptional switch in the adult fat body between metabolism and immunity (Clark et al., 2013). The function of the link between immune activation and loss of anabolic signaling activity is unclear in silkworm. In our study, immune response could affect the expression of a series of metabolic genes. These results suggests that bacterial invasion results in more energy consumption. However, some studies in *D. melanogaster* showed that blocking of the energy wasting extended the life span after infection with *Mycobacterium* and *Listeria* (Dionne et al., 2006, Chambers et al., 2012). These inconsistent results suggest that the interaction mechanism between immune response and metabolism response is not generally simple and needs further investigation.

In summary, we analyzed the transcriptome of the silkworm midgut after bacterial infection. Our data revealed that the silkworm midgut produces high level of ROS and AMPs sequentially to defend against ingested bacteria. We also discussed their regulatory mechanism and the possible involvement of the Toll pathway in the gut.

## Author contributions

ZL and ZZ designed the research; RW and KC preformed the research; RW, KC, LX, ZL, ZL and ZZ analyzed the data; ZL and ZZ wrote the manuscript. All authors read and approved the final manuscript.

## Funding

## Appendix A. Supplementary data

Supplementary data to this article can be found online at https://doi.org/10.1016/j.dci.2020.103720.

## References

Akira, S., Uematsu, S., Takeuchi, O., 2006. Pathogen recognition and innate immunity. Cell 124, 783–801.
Ardia, D.R., Gantz, J.E., Schneider, B.C., Strebel, S., 2012. Costs of immunity in insects: an induced immune response increases metabolic rate and decreases antimicrobial activity. Funct. Ecol. 26, 732–739.
Artis, D., 2008. Epithelial-cell recognition of commensal bacteria and maintenance of immune homeostasis in the gut. Nat. Rev. Immunol. 8, 411–420.
Ashburner, M., Ball, C.A., Blake, J.A., Botstein, D., Butler, H., Cherry, J.M., Davis, A.P., Dolinski, K., Dwight, S.S., Eppig, J.T., Harris, M.A., Hill, D.P., Issel-Tarver, L., Kasarskis, A., Lewis, S., Matese, J.C., Richardson, J.E., Ringwald, M., Rubin, G.M., Sherlock, G., 2000. Gene ontology: tool for the unification of biology. The Gene Ontology Consortium. Nat. Genet. 25, 25–29.
Bajgar, A., Kucerova, K., Jonatova, L., Tomcala, A., Schneedorferova, I., Okrouhlik, J., Dolezal, T., 2015. Extracellular adenosine mediates a systemic metabolic switch during immune response. PLoS Biol. 13, e1002135.
Becker, T., Loch, G., Beyer, M., Zinke, I., Aschenbrenner, A.C., Carrera, P., Inhester, J.L., Hoch, M., 2010. FOXO-dependent regulation of innate immune homeostasis. Nature 463, 369–373.
Buchon, N., Broderick, N.A., Lemaitre, B., 2013. Gut homeostasis in a microbial world: insights from *Drosophila melanogaster*. Nat. Rev. Microbiol. 119, 615–626.
Buchon, N., Broderick, N.A., Poidevin, M., Pradervand, S., Lemaitre, B., 2009. *Drosophila* intestinal response to bacterial infection: activation of host defense and stem cell proliferation. Cell Host Microbe 5, 200–211.
Bulet, P., Hetru, C., Dimarcq, J.L., Hoffmann, D., 1999. Antimicrobial peptides in insects; structure and function. Dev. Comp. Immunol. 23, 329–344.
Chambers, M.C., Song, K.H., Schneider, D.S., 2012. *Listeria monocytogenes* infection causes metabolic shifts in Drosophila melanogaster. PloS One 7, e50679.
Charroux, B., Royet, J., 2012. Gut-microbiota interactions in non-mammals: what can we

learn from *Drosophila*? Semin. Immunol. 24, 17–24.

Chen, K., Liu, C., He, Y., Jiang, H., Lu, Z., 2014. A short-type peptidoglycan recognition protein from the silkworm: expression, characterization and involvement in the prophenoloxidase activation pathway. Dev. Comp. Immunol. 45, 1–9.

Chen, K., Lu, Z., 2018. Immune responses to bacterial and fungal infections in the silkworm, *Bombyx mori*. Dev. Comp. Immunol. 83, 3–11.

Chen, K., Zhou, L., Chen, F., Peng, Y., Lu, Z., 2016. Peptidoglycan recognition protein-S5 functions as a negative regulator of the antimicrobial peptide pathway in the silkworm, *Bombyx mori*. Dev. Comp. Immunol. 61, 126–135.

Cheng, T., Lin, P., Huang, L., Wu, Y., Jin, S., Liu, C., Xia, Q., 2016. Genome-wide analysis of host responses to four different types of microorganisms in *Bombyx mori* (Lepidoptera: bombycidae). J. Insect Sci. 16.

Cheng, T., Zhao, P., Liu, C., Xu, P., Gao, Z., Xia, Q., Xiang, Z., 2006. Structures, regulatory regions, and inductive expression patterns of antimicrobial peptide genes in the silkworm *Bombyx mori*. Genomics 87, 356–365.

Chowdhury, S., Taniai, K., Hara, S., Kadono-Okuda, K., Kato, Y., Yamamoto, M., Xu, J., Choi, S.K., Debnath, N.C., Choi, H.K., Miyanoshita, A., Sugiyama, M., Asaoka, A., Yamakawa, M., 1995. cDNA cloning and gene expression of lebocin, a novel member of antibacterial peptides from the silkworm, *Bombyx mori*. Biochem. Biophys. Res. Commun. 214, 271–278.

Clark, R.I., Tan, S.W., Pean, C.B., Roostalu, U., Vivancos, V., Bronda, K., Pilatova, M., Fu, J., Walker, D.W., Berdeaux, R., Geissmann, F., Dionne, M.S., 2013. MEF2 is an in vivo immune-metabolic switch. Cell 155, 435–447.

DiAngelo, J.R., Bland, M.L., Bambina, S., Cherry, S., Birnbaum, M.J., 2009. The immune response attenuates growth and nutrient storage in *Drosophila* by reducing insulin signaling. Proc. Natl. Acad. Sci. U.S.A. 106, 20853–20858.

Dillon, R.J., Dillon, V.M., 2004. The gut bacteria of insects: nonpathogenic interactions. Annu. Rev. Entomol. 49, 71–92.

Dionne, M.S., Pham, L.N., Shirasu-Hiza, M., Schneider, D.S., 2006. Akt and FOXO dysregulation contribute to infection-induced wasting in *Drosophila*. Curr. Biol. 16, 1977–1985.

Dong, Y., Manfredini, F., Dimopoulos, G., 2009. Implication of the mosquito midgut microbiota in the defense against malaria parasites. PLoS Pathog. 5, e1000423.

Drenkard, E., Ausubel, F.M., 2002. Pseudomonas biofilm formation and antibiotic resistance are linked to phenotypic variation. Nature 416, 740–743.

Eleftherianos, I., Felfoldi, G., ffrench-Constant, R.H., Reynolds, S.E., 2009. Induced nitric oxide synthesis in the gut of *Manduca sexta* protects against oral infection by the bacterial pathogen *Photorhabdus luminescens*. Insect Mol. Biol. 18, 507–516.

Fang, F.C., 2004. Antimicrobial reactive oxygen and nitrogen species: concepts and controversies. Nat. Rev. Microbiol. 2, 820–832.

Foley, E., O'Farrell, P.H., 2003. Nitric oxide contributes to induction of innate immune responses to gram-negative bacteria in *Drosophila*. Genes Dev. 17, 115–125.

Freitak, D., Ots, I., Vanatoa, A., Horak, P., 2003. Immune response is energetically costly in white cabbage butterfly pupae. Proc. Biol. Sci. 270, S220–S222.

Furukawa, S., Tanaka, H., Nakazawa, H., Ishibashi, J., Shono, T., Yamakawa, M., 1999. Inducible gene expression of moricin, a unique antibacterial peptide from the silkworm (Bombyx mori). Biochem. J. 340 (Pt 1), 265–271.

Goldsmith, M.R., Shimada, T., Abe, H., 2005. The genetics and genomics of the silkworm, *Bombyx mori*. Annu. Rev. Entomol. 50, 71–100.

Grabherr, M.G., Haas, B.J., Yassour, M., Levin, J.Z., Thompson, D.A., Amit, I., 2011. Full-length transcriptome assembly from RNA-Seq data without a reference genome. Nat. Biotechnol. 29.

Ha, E.M., Oh, C.T., Bae, Y.S., Lee, W.J., 2005a. A direct role for dual oxidase in *Drosophila* gut immunity. Science 310, 847–850.

Ha, E.M., Oh, C.T., Ryu, J.H., Bae, Y.S., Kang, S.W., Jang, I.H., Brey, P.T., Lee, W.J., 2005b. An antioxidant system required for host protection against gut infection in *Drosophila*. Dev. Cell 8, 125–132.

Hara, S., Yamakawa, M., 1995. Moricin, a novel type of antibacterial peptide isolated from the silkworm, *Bombyx mori*. J. Biol. Chem. 270, 29923–29927.

Hoffmann, D., Hultmark, D., Boman, H.G., 1981. Insect immunity: *Galleria mellonella* and other lepidoptera have cecropia-P9-like factors active against gram negative bacteria. Insect Biochem. 11, 537–548.

Hoffmann, J.A., Reichhart, J.M., 2002. *Drosophila* innate immunity: an evolutionary perspective. Nat. Immunol. 3, 121–126.

Hotamisligil, G.S., 2006. Inflammation and metabolic disorders. Nature 444, 860–867.

Hou, C., Qin, G., Liu, T., Geng, T., Gao, K., Pan, Z., Qian, H., Guo, X., 2014. Transcriptome analysis of silkworm, *Bombyx mori*, during early response to Beauveria bassiana challenges. PLoS One 9, e91189.

Hu, C., Wang, F., Ma, S., Li, X., Song, L., Hua, X., Qia, Q., 2015. Suppression of intestinal immunity through silencing of TCTP by RNAi in transgenic silkworm, *Bombyx mori*. Gene 574, 82–87.

Hu, X., Yang, R., Zhang, X., Chen, L., Xiang, X., Gong, C., Wu, X., 2013. Molecular cloning and functional characterization of the dual oxidase (BmDuox) gene from the silkworm *Bombyx mori*. PLoS One 8, e70118.

Huang, L., Cheng, T., Xu, P., Cheng, D., Fang, T., Xia, Q., 2009. A genome-wide survey for host response of silkworm, *Bombyx mori* during pathogen *Bacillus bombysepticus* infection. PLoS One 4, e8098.

Hultmark, D., 2003. *Drosophila* immunity: paths and patterns. Curr. Opin. Immunol. 15, 12–19.

Ishii, M., Matsumoto, Y., Sekimizu, K., 2015. Usefulness of silkworm as a model animal for understanding the molecular mechanisms of fungal pathogenicity. Drug Discov. Ther. 9, 234–237.

Jiang, L., Peng, Z., Guo, Y., Cheng, T., Guo, H., Sun, Q., Huang, C., Zhao, P., Xia, Q., 2016. Transcriptome analysis of interactions between silkworm and cytoplasmic polyhedrosis virus. Sci. Rep. 6 24894.

Jones, R.M., Luo, L., Ardita, C.S., Richardson, A.N., Kwon, Y.M., Mercante, J.W., Alam, A.,

Gates, C.L., Wu, H., Swanson, P.A., Lambeth, J.D., Denning, P.W., Neish, A.S., 2013. Symbiotic lactobacilli stimulate gut epithelial proliferation via Nox-mediated generation of reactive oxygen species. EMBO J. 32, 3017–3028.

Joshua, G.W., Karlyshev, A.V., Smith, M.P., Isherwood, K.E., Titball, R.W., Wren, B.W., 2003. A *Caenorhabditis elegans* model of *Yersinia* infection: biofilm formation on a biotic surface. Microbiology 149 (Pt 11), 3221–3229.

Kaito, C., 2016. Understanding of bacterial virulence using the silkworm infection model. Drug Discov. Ther. 10, 30–33.

Kaneko, Y., Furukawa, S., Tanaka, H., Yamakawa, M., 2007. Expression of antimicrobial peptide genes encoding Enbocin and Gloverin isoforms in the silkworm, *Bombyx mori*. Biosci. Biotechnol. Biochem. 71, 2233–2241.

Kanost, M.R., Jiang, H., Yu, X.Q., 2004. Innate immune responses of a lepidopteran insect, *Manduca sexta*. Immunol. Rev. 198, 97–105.

Kato, Y., Taniai, K., Hirochika, H., Yamakawa, M., 1993. Expression and characterization of cDNAs for cecropin B, an antibacterial protein of the silkworm, *Bombyx mori*. Insect Biochem. Mol. Biol. 23, 285–290.

Knowles, R.G., Moncada, S., 1994. Nitric oxide synthases in mammals. Biochem. J. 298 (Pt 2), 249–258.

Koizumi, N., Imai, Y., Morozumi, A., Imamura, M., Kadotani, T., Yaoi, K., Iwahana, H., Sato, R., 1999. Lipopolysaccharide-binding protein of *Bombyx mori* participates in a hemocyte-mediated defense reaction against gram-negative bacteria. J. Insect Physiol. 45 (9), 853–859.

Kolliopoulou, A., Van Nieuwerburgh, F., Stravopodis, D.J., Deforce, D., Swevers, L., Smagghe, G., 2015. Transcriptome analysis of *Bombyx mori* larval midgut during persistent and pathogenic cytoplasmic polyhedrosis virus infection. PLoS One 10, e0121447.

Krause, K.H., 2007. Aging: a revisited theory based on free radicals generated by NOX family NADPH oxidases. Exp. Gerontol. 42, 256–262.

Kumar, S., Molina-Cruz, A., Gupta, L., Rodrigues, J., Barillas-Mury, C., 2010. A peroxidase/dual oxidase system modulates midgut epithelial immunity in *Anopheles gambiae*. Science 327, 1644–1648.

Lee, K.A., Lee, W.J., 2018. Immune-metabolic interactions during systemic and enteric infection in *Drosophila*. Curr. Opin. Insect Sci. 29, 21–26.

Lemaitre, B., Hoffmann, J., 2007. The host defense of *Drosophila* melanogaster. Annu. Rev. Immunol. 25, 697–743.

Ley, R.E., Lozupone, C.A., Hamady, M., Knight, R., Gordon, J.I., 2008. Worlds within worlds: evolution of the vertebrate gut microbiota. Nat. Rev. Microbiol. 6, 776–788.

Li, J., Ma, L., Lin, Z., Zou, Z., Lu, Z., 2016. Serpin-5 regulates prophenoloxidase activation and antimicrobial peptide pathways in the silkworm, *Bombyx mori*. Insect Biochem. Mol. Biol. 73, 27–37.

Li, X.S., Wang, G.B., Sun, Y., Liu, W., He, Y.Z., Wang, F.C., Jiang, Y.R., Qin, L., 2016. Transcriptome analysis of the midgut of the Chinese oak silkworm *Antheraea pernyi* infected with *Antheraea pernyi* nucleopolyhedrovirus. PLoS One 11, e0165959.

Li, W., Godzik, A., 2006. Cd-hit: a fast program for clustering and comparing large sets of protein or nucleotide sequences. Bioinformatics 22, 1658–1659.

Li, Y., Xiang, Q., Zhang, Q., Huang, Y., Su, Z., 2012. Overview on the recent study of antimicrobial peptides: origins, functions, relative mechanisms and application. Peptides 37, 207–215.

Ma, Z., Li, C., Pan, G., Li, Z., Han, B., Xu, J., Lan, X., Chen, J., Yang, D., Chen, Q., Sang, Q., Ji, X., Li, T., Long, M., Zhou, Z., 2013. Genome-wide transcriptional response of silkworm (*Bombyx mori*) to infection by the microsporidian Nosema bombycis. PLoS One 8, e84137.

Masuzzo, A., Royet, J., 2018. Lipid catabolism fuels *Drosophila* gut immunity. Cell Host Microbe 23, 288–290.

Nakajima, S., Kitamura, M., 2013. Bidirectional regulation of NF-kappaB by reactive oxygen species: a role of unfolded protein response. Free Radic. Biol. Med. 65, 162–174.

Nappi, A.J., Vass, E., Frey, F., Carton, Y., 2000. Nitric oxide involvement in *Drosophila* immunity. Nitric Oxide 4, 423–430.

Ochiai, M., Ashida, M., 1988. Purification of a beta-1,3-glucan recognition protein in the prophenoloxidase activating system from hemolymph of the silkworm, *Bombyx mori*. J. Biol. Chem. 263, 12056–12062.

Otho, S.A., Chen, K., Zhang, Y., Wang, P., Lu, Z., 2016. Silkworm ferritin 1 heavy chain homolog is involved in defense against bacterial infection through regulation of haemolymph iron homeostasis. Dev. Comp. Immunol. 55, 152–158.

Pan, X., Zhou, G., Wu, J., Bian, G., Lu, P., Raikhel, A.S., Xi, Z., 2012. *Wolbachia* induces reactive oxygen species (ROS)-dependent activation of the Toll pathway to control dengue virus in the mosquito *Aedes aegypti*. Proc. Natl. Acad. Sci. U.S.A. 109, E23–E31.

Pezzulo, A.A., Hornick, E.E., Rector, M.V., Estin, M., Reisetter, A.C., Taft, P.J., Butcher, S.C., Carter, A.B., Manak, J.R., Stoltz, D.A., Zabner, J., 2012. Expression of human paraoxonase 1 decreases superoxide levels and alters bacterial colonization in the gut of *Drosophila melanogaster*. PLoS One 7, e43777.

Ribeiro, J.M., Genta, F.A., Sorgine, M.H., Logullo, R., Mesquita, R.D., Paiva-Silva, G.O., Majerowicz, D., Medeiros, M., Koerich, L., Terra, W.R., Ferreira, C., Pimentel, A.C., Bisch, P.M., Leite, D.C., Diniz, M.M., da, S.G.V., Junior, J.L., Da Silva, M.L., Araujo, R.N., Gandara, A.C., Brosson, S., Salmon, D., Bousbata, S., Gonzalez-Caballero, N., Silber, A.M., Alves-Bezerra, M., Gondim, K.C., Silva-Neto, M.A., Atella, G.C., Araujo, H., Dias, F.A., Polycarpo, C., Vionette-Amaral, R.J., Fampa, P., Melo, A.C., Tanaka, A.S., Balczun, C., Oliveira, J.H., Goncalves, R.L., Lazoski, C., Rivera-Pomar, R., Diambra, L., Schaub, G.A., Garcia, E.S., Azambuja, P., Braz, G.R., Oliveira, P.L., 2014. An insight into the transcriptome of the digestive tract of the bloodsucking bug, *Rhodnius prolixus*. PLoS Neglected Trop. Dis. 8, e2594.

Ryu, J.H., Ha, E.M., Lee, W.J., 2010. Innate immunity and gut-microbe mutualism in *Drosophila*. Dev. Comp. Immunol. 34, 369–376.

Ryu, J.H., Ha, E.M., Oh, C.T., Seol, J.H., Brey, P.T., Jin, I., Lee, D.G., Kim, J., Lee, D., Lee,

W.J., 2006. An essential complementary role of NF-kappaB pathway to microbicidal oxidants in *Drosophila* gut immunity. EMBO J. 25, 3693–3701.

Sansonetti, P.J., 2004. War and peace at mucosal surfaces. Nat. Rev. Immunol. 4, 953–964.

Shu, M., Mang, D., Fu, G.S., Tanaka, S., Endo, H., Kikuta, S., Sato, R., 2016. Mechanisms of nodule-specific melanization in the hemocoel of the silkworm, *Bombyx mori*. Insect Biochem. Mol. Biol. 70, 10–23.

Singh, P.K., Parsek, M.R., Greenberg, E.P., Welsh, M.J., 2002. A component of innate immunity prevents bacterial biofilm development. Nature 417, 552–555.

Switala, J., Loewen, P.C., 2002. Diversity of properties among catalases. Arch. Biochem. Biophys. 401, 145–154.

Tanaka, H., Ishibashi, J., Fujita, K., Nakajima, Y., Sagisaka, A., Tomimoto, K., Suzuki, N., Yoshiyama, M., Kaneko, Y., Iwasaki, T., Sunagawa, T., Yamaji, K., Asaoka, A., Mita, K., Yamakawa, M., 2008. h. Insect Biochem. Mol. Biol. 38, 1087–1110.

Tzou, P., Ohresser, S., Ferrandon, D., Capovilla, M., Reichhart, J.M., Lemaitre, B., Hoffmann, J.A., Imler, J.L., 2000. Tissue-specific inducible expression of antimicrobial peptide genes in *Drosophila* surface epithelia. Immunity 13, 737–748.

Wang, G., Zhang, J., Shen, Y., Zheng, Q., Feng, M., Xiang, X., Wu, X., 2015. Transcriptome analysis of the brain of the silkworm *Bombyx mori* infected with *Bombyx mori* nucleopolyhedrovirus: a new insight into the molecular mechanism of enhanced locomotor activity induced by viral infection. J. Invertebr. Pathol. 128, 37–43.

Wang, L., Feng, Z., Wang, X., Wang, X., Zhang, X., 2010. DEGseq: an R package for identifying differentially expressed genes from RNA-seq data. Bioinformatics 26, 136–138.

Wang, J.-M., Cheng, Y., Shi, Z.-K., Li, X.-F., Xing, L.-S., Jiang, H., Wen, D., Deng, Y.-Q., Zheng, A.-H., Qin, C.-F., Zou, Z., 2019. *Aedes aegypti* HPX8C modulates immune responses against viral infection. PLoS Neglected Trop. Dis. 13, e0007287.

Wang, Q., Zhou, Y., Chen, K., Ju, X., 2016. Identification and characterization of an atypical 2-cys peroxiredoxin from the silkworm, *Bombyx mori*. Insect Mol. Biol. 25 (4), 347–354.

Wang, Y., Cheng, T., Rayaprolu, S., Zou, Z., Xia, Q., Xiang, Z., Jiang, H., 2007. Proteolytic activation of pro-spatzle is required for the induced transcription of antimicrobial peptide genes in lepidopteran insects. Dev. Comp. Immunol. 31, 1002–1012.

Wu, J., Mao, X., Cai, T., Luo, J., Wei, L., 2006. KOBAS server: a web-based platform for automated annotation and pathway identification. Nucleic Acids Res. 34, W720–W724 Web Server issue.

Wu, S., Zhang, X., Chen, X., Cao, P., Beerntsen, B.T., Ling, E., 2010a. BmToll9, an Arthropod conservative Toll, is likely involved in the local gut immune response in the silkworm, *Bombyx mori*. Dev. Comp. Immunol. 34, 93–96.

Wu, S., Zhang, X., He, Y., Shuai, J., Chen, X., Ling, E., 2010b. Expression of antimicrobial peptide genes in *Bombyx mori* gut modulated by oral bacterial infection and development. Dev. Comp. Immunol. 34, 1191–1198.

Xia, Q., Li, S., Feng, Q., 2014. Advances in silkworm studies accelerated by the genome

sequencing of *Bombyx mori*. Annu. Rev. Entomol. 59, 513–536.

Xie, C., Mao, X., Huang, J., Ding, Y., Wu, J., Dong, S., Kong, L., Gao, G., Li, C.Y., Wei, L., 2011. Kobas 2.0: a web server for annotation and identification of enriched pathways and diseases. Nucleic Acids Res. 39, W316–W322 Web Server issue.

Xiong, G.H., Xing, L.S., Lin, Z., Saha, T.T., Wang, C., Jiang, H., Zou, Z., 2015. High throughput profiling of the cotton bollworm *Helicoverpa armigera* immunotranscriptome during the fungal and bacterial infections. BMC Genom. 16, 321.

Xu, P.Z., Zhang, M.R., Cheng, T.C., Huang, L.L., Tan, X., Xia, Q.Y., 2010. Molecular cloning and expression profile analysis of genes encoding pattern recognition receptors PGRP and βGRP in the silkworm, *Bombyx mori*. Sci. Seric. (Q.) 36 (3) 0383-0390.

Xu, Q., Lu, A., Xiao, G., Yang, B., Zhang, J., Li, X., Guan, J., Shao, Q., Beerntsen, B.T., Zhang, P., Wang, C., Ling, E., 2012. Transcriptional profiling of midgut immunity response and degeneration in the wandering silkworm, *Bombyx mori*. PLoS One 7, e43769.

Yang, J., Furukawa, S., Sagisaka, A., Ishibashi, J., Taniai, K., Shono, T., Yamakawa, M., 1999. cDNA cloning and gene expression of cecropin D, an antibacterial protein in the silkworm, *Bombyx mori*. Comp. Biochem. Physiol. B Biochem. Mol. Biol. 122, 409–414.

Yang, W., Cheng, T., Ye, M., Deng, X., Yi, H., Huang, Y., Tan, X., Han, D., Wang, B., Xiang, Z., Cao, Y., Xia, Q., 2011. Functional divergence among silkworm antimicrobial peptide paralogs by the activities of recombinant proteins and the induced expression profiles. PLoS One 6, e18109.

Yang, P.J., Zhan, M.Y., Ye, C., Yu, X.Q., Rao, X.J., 2017. Molecular cloning and characterization of a short peptidoglycan recognition protein from silkworm *Bombyx mori*. Insect Mol. Biol. 26, 665–676.

Yoshida, H., Kinoshita, K., Ashida, M., 1996. Purification of a peptidoglycan recognition protein from hemolymph of the silkworm, *Bombyx mori*. J. Biol. Chem. 271 (23), 13854–13860.

Yue, Y.J., Tang, X.D., Xu, L., Yan, W., Li, Q.L., Xiao, S.Y., Fu, X.L., Wang, W., Li, N., Shen, Z.Y., 2015. Early responses of silkworm midgut to microsporidium infection–A Digital Gene Expression analysis. J. Invertebr. Pathol. 124, 6–14.

Zhan, M.Y., Yang, P.J., Rao, X.J., 2018. Molecular cloning and analysis of PGRP-L1 and IMD from silkworm *Bombyx mori*. Comparative biochemistry and physiology. Biochem. Mol. Biol. 215, 19–30.

Zhang, K., Tan, J., Xu, M., Su, J., Hu, R., Chen, Y., Xuan, F., Yang, R., Cui, H., 2014. A novel granulocyte-specific alpha integrin is essential for cellular immunity in the silkworm *Bombyx mori*. J. Insect Physiol. 71, 61–67.

Zhang, L., Lu, Z., 2015. Expression, purification and characterization of an atypical 2-Cys peroxiredoxin from the silkworm, *Bombyx mori*. Insect Mol. Biol. 24 (2), 203–212.

Zhang, L., Wang, Y.W., Lu, Z.Q., 2015. Midgut immune responses induced by bacterial infection in the silkworm, *Bombyx mori*. J. Zhejiang Univ. - Sci. B. 16, 875–882.